JOURNAL OF CATALYSIS **101**, 103–113 (1986)

Acidic Properties of Binary Oxide Catalysts

I. Mössbauer Spectroscopy and Pyridine Adsorption for Iron Supported on Silica

GLEN CONNELL[1] AND J. A. DUMESIC[2]

Department of Chemical Engineering, University of Wisconsin, Madison, Wisconsin 53706

The acidic properties of 0.5 and 1.0 wt% iron supported on silica were probed by adsorption of pyridine, as studied by gravimetric measurements and infrared spectroscopy. The state of iron on silica was monitored by Mössbauer spectroscopy. This latter technique showed evidence for three types of Fe cations on the surface of silica, i.e., trivalent iron and two states of divalent iron having low and high coordination, respectively. Addition of iron to the silica generated Lewis acid sites on the surface, while little or no acidity existed on the silica surface alone. These new acid sites were shown to be iron cations in sites of low coordination. Infrared spectroscopy and gravimetric measurements of adsorbed pyridine indicated that the trivalent iron cations were stronger Lewis acids than divalent iron cations. The strength differences of the different oxidation states is explained on the basis of electronegativity differences. © 1986 Academic Press, Inc.

INTRODUCTION

Understanding the acidic properties of metal oxides is an important step toward the effective utilization of these materials in adsorptive and catalytic processes. Indeed, there is special interest in the properties of mixed metal oxides because of the ability to vary the acidic properties of these materials by choosing different metal oxide constituents at different concentrations (*1, 2*). In general, however, the materials prepared from arbitrary combinations of metal oxides may have complex structures. For example, the material may not be monophasic or of uniform composition. This has slowed progress in understanding the acidic properties of these materials. For this reason, a study was undertaken of acid sites on model, binary oxides formed by doping one metal oxide at low concentrations onto the surface of a second metal oxide. Conceptually, in the limit of dilute binary oxides the major component controls the oxide structure and the dopant surface concentration controls the number of new acid sites. In the present paper, the acidic properties of iron oxide supported on silica will be reported. In a second paper (*3*), the acidic properties of iron oxide will be examined on a series of different oxide supports (Al_2O_3, TiO_2, MgO); and, in a subsequent paper (*4*), the acidic properties of a series of different metal cations on silica will be studied. Throughout these studies we will attempt to relate the strength and type (i.e., Lewis versus Brønsted) of the acid sites to the nature of the dopant metal cation and the properties and structure of the oxide support.

It has been shown previously in the literature that one can generate new acid sites on the surface of a metal oxide by adding small amounts of a second oxide, with essentially one new acid site formed for each added cation (*5–7*). It is generally assumed, for example, that Lewis acidity is generated by the formation of coordinatively unsaturated metal cations on the surface. For the case of iron oxide supported on silica, it has

---

[1] Present address: 3M Center, St. Paul, Minn. 55144.

[2] To whom correspondence should be addressed.

0021-9517/86 $3.00

also been shown by Mössbauer spectroscopy that iron cations of low coordination are present at iron loadings typically lower than 1 wt% (e.g., Refs. (*8–11*)). In addition, it has been demonstrated that ammonia adsorbs on these coordinatively unsaturated iron cations (*9*). Thus, materials prepared by doping iron onto silica should provide a useful basis for probing the acidic properties of metal cations on surfaces, since the iron cations have been shown to be acidic and Mössbauer spectroscopy can be used to monitor the chemical state and coordination of these iron cations on the surface. This is the strategy of the present paper.

A variety of techniques can be used to study the acidic properties of solid surfaces (e.g., Refs. (*1, 2, 12*)). For example, the number and strength of acid sites have been titrated using Hammett indicators. The catalytic properties of these sites have been studied by measuring rates and selectivities of reactions catalyzed by acid sites. Importantly, the number, strength and type of acid sites have also been probed by studying the adsorption of basic molecules. The present study utilizes the latter method to study the acidic properties of iron cations supported on silica. Pyridine is the basic molecule used to probe the acid sites. Gravimetric measurements of the amount of adsorbed pyridine at different temperatures are used to determine the number of acid sites, and infrared spectroscopy of the adsorbed pyridine is employed to determine the nature of the acid sites and to probe the strength of these sites.

EXPERIMENTAL

Sample Preparation

Samples were prepared by incipient wetness impregnation. One cm^3 of an iron(III) nitrate solution (Alfa Ventron 99.999%) was added dropwise per gram of silica (Cab-O-Sil, Grade S-17). The concentration of the impregnation solution was adjusted to give an iron loading of either 0.5 or 1.0 wt%. The samples were then treated at 400 K in air for 24 h. Samples were subsequently treated in the appropriate apparatus for the measurement of pyridine adsorption, as described below.

Mössbauer Spectroscopy

Samples for Mössbauer spectroscopy studies were made utilizing iron enriched with ^{57}Fe. Samples used contained 0.5 wt% Fe. They were pressed into 250-mg pellets and placed into a quartz holder in a Mössbauer cell described previously (*13*). Samples were then treated in flowing gases and spectra were subsequently collected at room temperature in 250 kPa of the treatment gas.

All spectra were computer-fit using a modified version of MFIT (*14*). The spectrometer was calibrated with a sodium nitroprusside standard. All spectra are reported relative to metallic iron at room temperature. The Mössbauer spectroscopy cell utilizes Be windows which contain an iron impurity. This has been accounted for by fitting the spectra with an additional doublet for this iron impurity. The doublet has been fit by constraining the peak positions to be equal to those determined from Mössbauer spectra of the windows alone, but allowing the dip and width of these peaks to vary. However, the final best fit was obtained after constraining the doublet due to Fe in Be windows to be the same for all spectra taken with the same sample. This window spectrum has been numerically subtracted from all the spectra shown here.

Gravimetric Adsorption Measurements

Pellets formed from 400 mg of Fe/SiO_2 were pressed and then placed in the pan of a quartz spring balance (Worden). The balance was connected to a diffusion-pumped glass system which achieved an ultimate dynamic pressure of 10^{-6} Torr (1 Torr = 133.3 Pa). In addition to the diffusion pump, a molecular sieve (13X) trap held at 77 K was positioned close to the sample.

Reduction and oxidation treatments were carried out by passing the appropriate gasses through the balance system. Hydrogen was purified by passage through a Deoxo unit (Engelhard) followed by a molecular sieve trap (13X) held at 77 K. The oxygen was purified by passage through a molecular sieve trap held at 195 K.

The sample was treated in three different ways to produce different types of surfaces. The initial treatment consisted of reduction in flowing H_2 at 673 K for 4 h followed by evacuation for 1 h to a pressure of 5×10^{-5} Torr. After this initial treatment, two subsequent treatments were carried out: (i) oxidation in O_2 at 423 K for 1 h followed by reduction in H_2 at 498 K for 4 h; and (ii) oxidation in O_2 at 423 K for 1 h. After treatment, the sample was evacuated at the last treatment temperature to a pressure of 5×10^{-5} Torr, cooled in vacuum to 423 K, and allowed to equilibrate with pyridine at 423 K. Pyridine (Mallinckrot Spectrophotometric Grade) was purified by storage over activated molecular sieve (13X) in a glass bulb connected to the apparatus. The pyridine was degassed by repetitive freeze–pump–thaw cycles. The pyridine was then kept at 273 K in an ice bath prior to and during adsorption. This gives a partial pressure of pyridine of 4.8 Torr. After the sample was allowed to come to equilibrium with pyridine for 1 h, it was subsequently evacuated until the ionization gauge located near the entrance to the diffusion pump had reached a pressure of 3×10^{-5} Torr. Because pyridine physisorbs strongly to many surfaces including the glass walls of the apparatus, this evacuation was carried out overnight (However, this pressure was reached after 5 h of evacuation.) The sample was then heated successively to 523, 623, and 673 K, with evacuation to a pressure of 3×10^{-5} Torr at each temperature. The sample weight was measured at each temperature. The weight as well as infrared spectroscopy evidence (to be presented later) indicate that all the adsorbed pyridine had desorbed after evacuation at 673 K.

Infrared Spectroscopy

Infrared spectra were collected using a Nicolet 7199 Fourier transform infrared spectrometer operated with a spectral resolution of 1 cm^{-1}. All spectra were collected at beam temperature (ca. 310 K).

The samples were pressed into a wafer with a density of 55 mg/cm^2 and placed into a stainless-steel holder which fits in a heatable IR cell. The cell consists of a section of Pyrex glass where the sample is held during high-temperature treatments and an aluminum section containing CaF_2 windows where the sample is held during collection of IR spectra. The sample is moved between these two sections along a stainless-steel track. The IR cell also contains a molecular sieve (13X) trap held at 77 K to aid in the evacuation of pyridine.

The samples were treated in flowing gasses for 4 h using the same conditions as for the gravimetric adsorption measurements. Prior to the adsorption of pyridine a background IR spectrum was collected, and this spectrum has been subtracted from all of the spectra shown here. The pyridine was then adsorbed at 423 K for 0.5 h followed by evacuation of the sample at 423 K for 0.5 h. At this point the pressure of pyridine was ca. 1×10^{-3} Torr. Helium (ca. 400 Torr) was admitted to the cell as a heat transfer medium and the sample cooled to room temperature prior to collecting a spectrum. The sample was then reheated to 423 K in He and evacuated for an additional 0.75 h, which reduced the pressure of pyridine to 1×10^{-4} Torr. An IR spectrum was then collected after cooling the sample at this point. The sample was subsequently evacuated at 523, 623, and 673 K to a pressure of 1×10^{-4} Torr and additional spectra collected after each evacuation.

RESULTS

Mössbauer Spectroscopy

Initial reduction of the 0.5 wt% Fe/SiO_2 sample at 673 K followed by oxidation of the sample at 423 K led to the spectrum

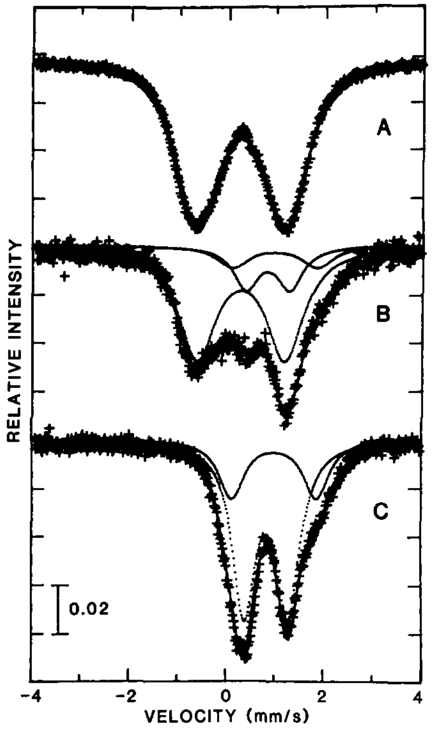

FIG. 1. Room-temperature Mössbauer spectra for 0.5 wt% Fe/SiO_2: (A) after reduction in H_2 at 673 K followed by oxidation in O_2 at 423 K; (B) after reduction in H_2 at 498 K; (C) after reduction in H_2 at 673 K.

shown in Fig. 1A. The Mössbauer parameters are listed in Table 1. This spectrum has been fit with a single Fe^{3+} doublet. The broadness and unequal areas of the two peaks are not fit exactly with one doublet; however, fitting the spectrum with additional peaks does not seem justifiable. The quadrupole splitting is high for Fe^{3+}, indicating that the cations are in sites of high distortion. In addition, the peaks are broad, indicating that there is a distribution of sites in which the Fe^{3+} is bonded to SiO_2.

Reduction of the sample at 498 K for 4 h in H_2 produced the spectrum shown in Fig. 1B. Here it can be seen that much of the Fe^{3+} remains, but some Fe^{2+} also appears in the spectrum. Reduction of the sample at 673 K led to the spectrum shown in Fig. 1C, according to which all of the iron is present as Fe^{2+}. The spectral contributions from Fe^{2+} in both Figs. 1B and C were fit with two doublets, the parameters of which are given in Table 1. Indeed, the rationale for fitting Fe^{2+} with two doublets has been discussed in the literature (e.g., Refs. (*8–11*)). These two doublets have been denoted as the inner and outer doublets. The inner doublet, with the smaller isomer shift and quadrupole splitting, has been assigned to Fe^{2+} cations in sites of low coordination. That is, they are bonded to the SiO_2 surface yet they are also coordinatively unsaturated. Hence they are accessible to the gas phase and are capable of adsorbing molecules. Making the assumption that the γ-ray absorption factors are equal for all iron phases one can estimate that about 70% of the Fe on the sample is in the low coordination state after reduction at 673 K. The outer doublet has a higher isomer shift and quadrupole splitting and has been assigned to Fe^{2+} cations in sites of higher coordination. They are essentially saturated with respect to ligands. These assignments are based on work in which H_2O, NH_3, methanol (*9*), and NO (*8*) were adsorbed onto the surface resulting in changes in the Mössbauer spectrum. Methanol, water, and ammonia converted inner doublet to outer doublet upon adsorption, i.e., low coordination Fe was converted to high coordination Fe upon adsorption of these molecules. The initial outer doublet and the new outer doublet formed upon adsorption are indistinguishable. Apparently, Mössbauer spectroscopy is not sufficiently sensitive to separate the two high coordination states of iron. This is also the case for Fe^{3+} spectra, which do not vary much for Fe on various oxides or for adsorption of gas-phase species. The insensitivity of Fe^{3+} may be a result of its half-filled *d*-shell which leaves only lattice contributions to the quadrupole splitting. Divalent iron, on the other hand, has six *d*-electrons and hence the quadrupole splitting has contributions both from the valence electrons as well as the lattice point charges.

Mössbauer spectra were collected at 6 K for two samples to examine further the

TABLE 1

Mössbauer Parameters for Spectra of 0.5 wt% Fe/SiO$_2$ Shown in Fig. 1

Species		Treatment gas and temperature		
		O$_2$, 423 K	H$_2$, 498 K	H$_2$, 673 K
Fe^{3+}				
Isomer shift	0.29 mm/s			
Quadrupole splitting	1.81 mm/s			
Fractional area		1.00	0.70	
Linewidth (mm/s)		1.08	0.92	
Area (pct. * mm/s)		23.09	13.11	
Fe^{2+} inner doublet				
Isomer shift	0.83 mm/s			
Quadrupole splitting	0.91 mm/s			
Fractional area			0.18	0.72
Linewidth (mm/s)			0.92	0.58
Area (pct. * mm/s)			3.41	12.43
Fe^{2+} outer doublet				
Isomer shift	0.98 mm/s			
Quadrupole splitting	1.74 mm/s			
Fractional area			0.12	0.28
Linewidth (mm/s)			0.77	0.64
Area (pct. * mm/s)			2.22	4.74

state of iron on the silica surface. One sample was reduced at 673 K in H$_2$ and the other sample was reduced in H$_2$ at 673 K followed by oxidation at 295 K in O$_2$. Neither spectrum showed evidence for any sextuplet which would occur for large, magnetic particles. One can estimate that if any Fe$_2$O$_3$ particles are present after oxidation, they must be less than about 3 nm in diameter (*15*). Hence, the iron must be spread over the SiO$_2$ surface in a highly dispersed form. Furthermore, reduction of Fe at 673 K in H$_2$ should produce metallic iron based on thermodynamic and kinetic data for iron in the absence of silica (e.g., Refs. (*16, 17*)). This is not observed, indicating that there is a strong interaction between Fe and the silica surface.

Three treatments were employed in this study to vary the relative amounts of the different types of iron on the surface. These treatments were oxidation at 423 K, reduction at 498 K, and reduction at 673 K. Each treatment varied the amount of Fe^{3+}, Fe^{2+} inner doublet, and Fe^{2+} outer doublet. The acidity of samples treated in the three different ways was then measured to determine the relative acidic properties of these three types of Fe.

The fully reduced sample (reduction at 673 K) was subjected to a gas stream of H$_2$ containing 4.8 Torr of pyridine at 423 K for 1 h followed by degassing of the sample in H$_2$ for 4 h at 423 K. The resulting spectrum is shown in Fig. 2A, with the Mössbauer parameters tabulated in Table 2. It can be seen that conversion of the Fe^{2+} inner doublet to outer doublet has occurred. In terms of spectral area, about 50% of the iron in the sample is altered by the adsorption of pyridine. As will be seen, this correlates well with the gravimetric adsorption measurements which show that 50% of the Fe^{2+} cations are acidic. Hence the assumption of equal recoil-free fractions for all spectral components is justified. Thus, low coordination iron has been converted to high coordination iron upon adsorption of pyri-

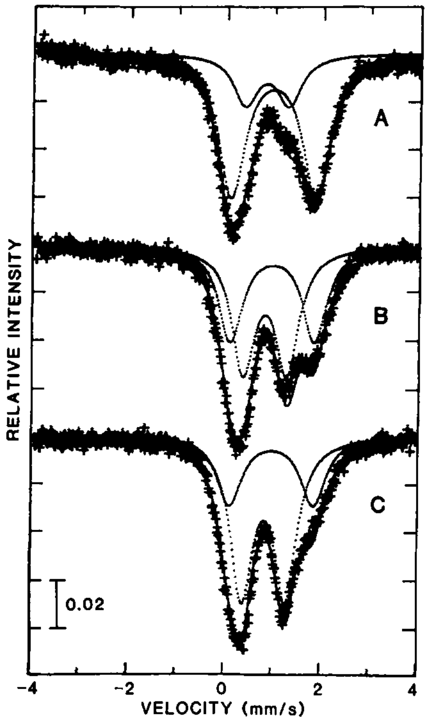

FIG. 2. Room-temperature Mössbauer spectra of 0.5 wt% Fe/SiO_2 after adsorption of pyridine: (A) after reduction in H_2 at 673 K followed by pyridine adsorption in H_2 at 423 K for 1 h and degassing in H_2 at 423 K for 4 h; (B) after degassing in H_2 at 523 K for 4 h; (C) after degassing in H_2 at 623 K for 4 h.

dine, and Mössbauer spectroscopy thereby demonstrates that the Fe^{2+} cations in low coordination are acid sites. As will be seen with the gravimetric adsorption measurements, there is a distribution of acid site strengths of these low coordination Fe^{2+} cations. The amorphous character of the SiO_2 surface should lead to a variety of different bonding sites for Fe on the surface. Hence not all the low coordination iron is apparently of sufficient acid strength to chemisorb pyridine at 423 K. Desorption of pyridine at 523 and 623 K results in spectra B and C (Fig. 2). The original Mössbauer spectrum is obtained after desorption at 673 K. Thus, the pyridine adsorption does not alter the dispersion or reconstruct the Fe on the sample, but rather it adsorbs on the iron cations and then desorbs at higher temperatures.

Mössbauer spectra after adsorption of pyridine on the partially reduced samples showed the same conversion of inner doublet to outer doublet but the effect was reduced because of the lesser amount of the Fe^{2+} inner doublet. Pyridine adsorption had no major effect on the Fe^{3+} spectrum. This does not necessarily mean that adsorption

TABLE 2

Mössbauer Parameters for Spectra of 0.5 wt% Fe/SiO_2 after Pyridine Adsorption Shown in Fig. 2

Species		Degassing temperature		
		423 K	523 K	623 K
Fe^{2+} inner doublet				
Isomer shift	0.83 mm/s			
Quadrupole splitting	0.91 mm/s			
Fractional area		0.24	0.55	0.67
Linewidth (mm/s)		0.62	0.59	0.53
Area (pct. * mm/s)		3.97	9.27	11.37
Fe^{2+} outer doublet				
Isomer shift	0.98 mm/s			
Quadrupole splitting	1.74 mm/s			
Fractional area		0.76	0.45	0.33
Linewidth (mm/s)		0.68	0.62	0.62
Area (pct. * mm/s)		12.40	7.64	5.60

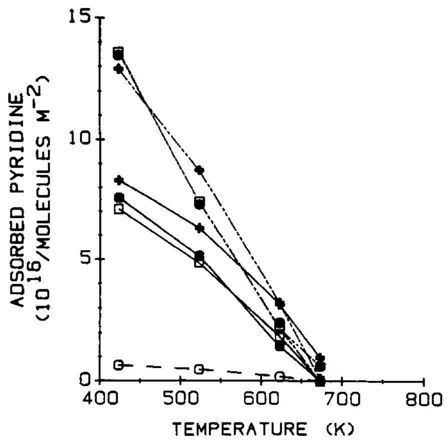

FIG. 3. Gravimetric measurements of pyridine adsorption on 1.0 and 0.5 wt% Fe/SiO_2: (●, dashed line) 1.0 wt% Fe/SiO_2 after reduction in H_2 at 673 K; (□, dashed line) 1.0 wt% Fe/SiO_2 after reduction in H_2 at 498 K; (+, dashed line) 1.0 wt% Fe/SiO_2 after reduction in H_2 at 673 K followed by oxidation in O_2 at 423 K; (+, solid line) 0.5 wt% Fe/SiO_2 after reduction in H_2 at 673 K followed by oxidation in O_2 at 423 K; (●, solid line) 0.5 wt% Fe/SiO_2 after reduction in H_2 at 673 K; (□, solid line) 0.5 wt% Fe/SiO_2 after reduction in H_2 at 498 K; (○) SiO_2 after reduction in H_2 at 673 K.

does not occur on Fe^{3+}, but rather that Mössbauer spectroscopy is not sensitive to this phenomenon.

Gravimetric Adsorption Measurements of Pyridine

Gravimetric measurements of pyridine adsorption are consistent with the Mössbauer spectroscopy data. The results on SiO_2 as well as for the three treatments of Fe/SiO_2 for two different Fe loadings of 0.5 and 1.0 wt% are shown in Fig. 3. The curve for SiO_2 (the lowest one) shows a minor amount of adsorption, barely within experimental detectability. The addition of Fe on SiO_2 increases the adsorption of pyridine. All three treatments give approximately the same number of sites for the 0.5 wt% sample. The amount of adsorption at 423 K corresponds to 50% of the added iron, which is what was observed for the conversion of inner doublet to outer doublet in the Mössbauer spectra. The data show that the two reduced samples exhibit essentially the same behavior toward pyridine adsorption. The oxidized sample, however, may show slightly more adsorption of pyridine. The difference between the reduced and oxidized samples is constant over the entire temperature range indicating that there might be an error in the initial weight of this sample. Hence, the enhanced acidity of the oxidized sample over the reduced samples may not be real, but the overall acidity of Fe/SiO_2 over SiO_2 is clear.

The results for the 1.0 wt% Fe/SiO_2 sample confirm the above findings, as seen in Fig. 3. Specifically, the 1.0 wt% sample shows twice the number of sites at the 423 K evacuation temperature as the 0.5 wt% sample, confirming that 50% of the Fe atoms generate acid sites. As with the 0.5 wt% sample, the two reduced samples are indistinguishable and the oxidized sample appears to show adsorption at the higher evacuation temperatures.

Infrared Spectroscopy of Adsorbed Pyridine

Infrared spectroscopy of adsorbed pyridine was used to determine the acid type and to probe the acid strength. The expected absorption frequencies for pyridine adsorbed on acid surfaces are shown in Table 3. Infrared spectra for pyridine adsorbed on oxidized Fe/SiO_2, fully reduced Fe/SiO_2 and SiO_2 are shown in Fig. 4, with

TABLE 3

Absorption Frequencies for Pyridine[a]

Mode[b]	Frequency (cm^{-1})			
	Liquid	HPY[c]	LPY[d]	BPY[e]
19b	1439	1440–1445	1445–1460	1530–1550
19a	1478	1480–1490	1478–1490	1478–1490
8b	1572	1577	1575–1585	1600–1613
8a	1579	1580–1600	1602–1632	1631–1640

[a] Adapted from Ref. (*18*).
[b] Modes as assigned by Ref. (*19*).
[c] Hydrogen-bonded pyridine.
[d] Pyridine bonded to a Lewis acid.
[e] Pyridine bonded to a Brønsted acid.

TABLE 4

Infrared Absorption Frequencies for Spectra of Pyridine Adsorbed on 0.5 wt% Fe/SiO_2 and SiO_2 Shown in Fig. 4

Sample	Fe/SiO_2	Fe/SiO_2	SiO_2
Treatment gas	O_2	H_2	H_2
Treatment temperature (K)	423	673	673
Pyridine desorption temperature (K)	523	523	523
Pyridine desorption pressure (Torr)	1×10^{-4}	2×10^{-4}	1×10^{-4}
Band	Absorption frequency (cm^{-1})		
19b	1453	1451	1446
19a	1491	1491	
8b		1576	1581
8a	1613	1610	1598

the frequencies listed in Table 4. These spectra are after adsorption of pyridine at 423 K and evacuation at 523 K to a pressure of less than 2×10^{-4} Torr. There are two major bands for silica (spectrum C) at 1446 and 1597 cm^{-1}. These correspond to the 19b and 8a bands of pyridine physisorbed on the surface. The iron-containing samples show similar spectra. Spectrum A is for an oxidized sample treated in O_2 at 423 K. The major bands occur at 1453 and 1613 cm^{-1}, indicative of Lewis acid sites. Spectrum B is for a fully reduced sample, i.e., treated in H_2 at 673 K. The major peaks occur at 1451 and 1610 cm^{-1}. These peaks also correspond to the 19b and 8a bands for pyridine adsorbed on Lewis acid sites. The strength of the Lewis acid sites for Fe^{2+} and Fe^{3+}

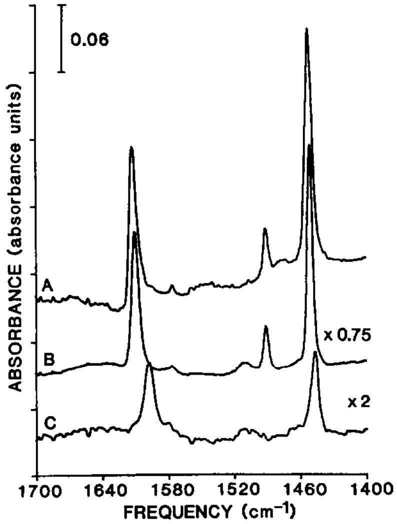

FIG. 4. Infrared spectra of pyridine adsorbed on 0.5 wt% Fe/SiO_2: (A) reduced in H_2 at 673 K followed by oxidation in O_2 at 423 K, pyridine desorbed at 523 K to a pressure of 1×10^{-4} Torr; (B) reduced in H_2 at 673 K, pyridine desorbed at 523 K to a pressure of 2×10^{-4} Torr; (C) SiO_2 reduced in H_2 at 673 K, pyridine desorbed at 523 K to a pressure of 1×10^{-4} Torr.

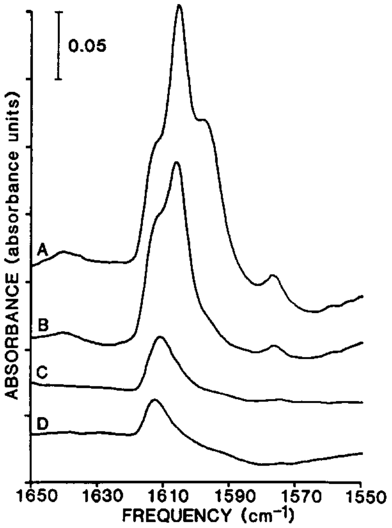

FIG. 5. Infrared spectra of the 8a band for pyridine adsorbed on 0.5 wt% Fe/SiO_2 after reduction in H_2 at 498 K. Evacuation temperature and pressure: (A) 423 K, 1×10^{-3} Torr; (B) 423 K, 2×10^{-4} Torr; (C) 523 K, 1×10^{-4} Torr; (D) 623 K, 1×10^{-4} Torr.

TABLE 5

Infrared Absorption Frequencies of the 8a Band for Pyridine Adsorbed on 0.5 wt% Fe/SiO_2 Treated in H_2 at 498 K Shown in Fig. 5

Pyridine desorption: temperature (K); Pressure (Torr)	Absorption frequency (cm^{-1})		
423; 1×10^{-3}	1612	1606	1598
423; 2×10^{-4}	1611	1606	—
523; 1×10^{-4}	1611	—	—
623; 1×10^{-4}	1612	—	—

may be different, however, as discussed below.

The Mössbauer spectra demonstrated that a sample reduced in H_2 at 498 K contains both Fe^{2+} and Fe^{3+} on the surface. Indeed, infrared spectra of pyridine adsorbed on such a sample exhibited distinct bands for both types of iron. The infrared spectra for the 8a band for a sample reduced in H_2 at 498 K are depicted in Fig. 5, with the absorption frequencies listed in Table 5. These spectra are after pyridine adsorption at 423 K followed by evacuation. Spectrum A is after evacuation at 423 K to a pressure of 1×10^{-3} Torr. As can be seen, there are three distinct peaks at 1612, 1606, and 1598 cm^{-1}. These frequencies correspond to the 8a peaks observed under similar conditions for pyridine adsorbed on Fe^{3+}, Fe^{2+}, and SiO_2, respectively. It should be noted that as the evacuation temperature is increased and as the evacuation pressure is decreased the bands shift upward in wavenumber. This is particularly true for Fe^{2+}, for which the band positions are at 1606 cm^{-1} at 423 K evacuation but at 1610 cm^{-1} at 523 K. Evacuation of the sample at 423 K to a pressure of 2×10^{-4} Torr gives spectrum B. Here the band for the physisorbed pyridine on SiO_2 has been removed, leaving only bands at 1611 and 1606 cm^{-1}. Evacuation of the sample at 523 K to a pressure of 1×10^{-4} Torr gives spectrum C. In this case, the band at 1606 has been removed leaving only a peak at 1611 cm^{-1}. Finally spectrum D is after evacuation at 623 K to a pressure of 1×10^{-4} Torr. Here the peak maximum occurs at 1612 cm^{-1}. This desorption series thus shows that on the partially reduced sample pyridine is physisorbed on silica and chemisorbed on Fe^{2+} and Fe^{3+}. The species desorb in the order listed above as the evacuation becomes more severe. This is evidence that the acid strength decreases in the following order:

$$Fe^{3+} > Fe^{2+} \gg SiO_2$$

It is thus demonstrated that the same element in a different oxidation state can have different acid strengths.

The above ordering of acid strength is consistent with the gravimetric studies of pyridine adsorption on the Fe/SiO_2 samples. In addition, it may be suggested that the frequency of the 8a infrared band of adsorbed pyridine can be correlated with acid strength. Specifically, the frequency of this band increases with increasing strength of pyridine adsorption (i.e., with increasing Lewis acid strength).

DISCUSSION

The generation of acid sites on the surface of silica upon doping the surface with iron has been demonstrated. The existence of new acid sites is proven with gravimetric adsorption measurements of pyridine. The amount of pyridine adsorbed on the Fe-containing samples after evacuation at 423 K corresponds to 50% of the added Fe.

The types of acid sites were shown by infrared spectroscopy to be Lewis acids. There was no evidence for Brønsted acid sites. This is in contrast to the work of Iizuka *et al.* (*20*) who found that their coprecipitated Fe/SiO_2 samples contained Brønsted acid sites. Our preparation method may not produce the types of bondings sites required to induce Brønsted acidity. Brønsted acidity has also been observed for Fe in the framework of ZSM-5 zeolite (*21*). In the zeolite, iron is in a tetrahedral framework site which, in general, is not expected to occur on our samples, as discussed below.

Lewis acids are electron pair acceptors, and on metal cations they have often been described as coordinatively unsaturated cations. The Mössbauer spectra prove that the pyridine adsorbs onto iron cations. The change of isomer shift and quadrupole splitting for the inner doublet Fe^{2+} cations when they are converted to outer doublet Fe^{2+} cations upon adsorption of pyridine indicates that pyridine is bonded directly to the iron cations.

The inner doublet cations have been assigned previously to low coordination sites (e.g., Refs. (*8–10*)). These assignments are based on the ability of the low coordination cations to convert to high coordination cations upon adsorption of methane, water, ammonia, and NO. This behavior is extended to include pyridine in the present study. The low coordination Fe^{2+} cations are observed only on a select number of oxides such as SiO_2 (*8–11*), TiO_2 (*5*), mordenite (*22*), Y-zeolite (*23–25*), L-zeolite (*26*), and A-zeolite (*27*). All of these solids have a structure which may allow for electrical neutrality yet leave the cations coordinatively unsaturated. In all of these oxides the coordination of oxygen is low (two for SiO_2 and the zeolites, and three for TiO_2). One can use Pauling's electrostatic bond strength rules (*28*) to predict a coordination of two for Fe^{2+} in a SiO_2 matrix to provide for charge neutrality. Even though a coordination of two may be unrealistically low, coordinatively unsaturated Fe^{2+} cations may thus be expected on silica.

It is proposed that the Lewis acid sites on the surface of Fe/SiO_2 are these low coordination Fe cations. The change in spectral area for conversion of inner doublet Fe^{2+} to outer doublet Fe^{2+} upon adsorption of pyridine at 423 K corresponds to 50% of the iron. This fraction is the same as observed with the gravimetric adsorption measurements. It is interesting to compare that when iron is forced into tetrahedral coordination in the structural framework of zeolites, protons must be added for electrical neutrality and Brønsted acid sites are created (*21*).

The number of Lewis acid sites on silica was found to be equal for Fe in both the divalent and trivalent oxidation states. This equality indicates that even in the trivalent state the iron cations remain coordinatively unsaturated. The high distortion of the coordination sphere around Fe^{3+} is confirmed with Mössbauer spectroscopy. The quadrupole splitting of 1.81 mm/s is high for Fe^{3+}. Hence the existence of coordinatively unsaturated Fe^{3+} cations is consistent with the Mössbauer spectra.

The strength of pyridine adsorption is higher on Fe^{3+} than on Fe^{2+}. This was indicated by infrared spectroscopy on the partially reduced sample which showed successive desorption of pyridine from the SiO_2, Fe^{2+} and Fe^{3+}, respectively, upon continued evacuation. This order of adsorption strengths is consistent with the gravimetric adsorption data and IR frequency shifts observed in this study. Indeed, the conclusion that Fe^{3+} is a stronger Lewis acid site than Fe^{2+} is in agreement with electronegativity arguments. For two cations in similar coordinations and bonding sites, one would expect the cation with higher electronegativity to be a stronger Lewis acid site. Trivalent iron is more electronegative than divalent iron and hence Fe^{3+} is a stronger acid.

CONCLUSIONS

The generation of new acid sites on the surface of SiO_2 upon addition of Fe has been demonstrated using pyridine adsorption. The acid sites are of the Lewis type, and they are shown to be associated with iron cations in sites of low coordination.

The number of acid sites is the same for Fe in either the divalent or trivalent oxidation states. Apparently oxidation of Fe^{2+} to Fe^{3+}, which requires addition of one oxygen anion for every two Fe^{2+} cations, does not complete the coordination of Fe^{3+}.

Hence, Fe^{3+} remains coordinatively unsaturated and acidic. The acid strength of Fe^{3+} is higher than Fe^{2+}, as expected in view of the higher electronegativity of the former cation.

ACKNOWLEDGMENTS

One of us (G.C.) would like to thank Amoco for providing a fellowship during this study. Support for this work was provided by the Office of Basic Energy Sciences of the Department of Energy (DE-FG02-84ER13183), and it is gratefully acknowledged.

REFERENCES

1. Tanabe, K., *in* "Catalysis Science and Technology" (J. R. Anderson and M. Boudart, Eds.), Vol. 2, p. 231. Springer-Verlag, New York, 1981.
2. Tanabe, K., "Solid Acids and Bases." Academic Press, New York, 1970.
3. Connell, G., and Dumesic, J. A., *J. Catal.*, in press.
4. Connell, G., and Dumesic, J. A., submitted for publication.
5. Murrell, L. L., and Garten, R. L., *Appl. Surf. Sci.* **19,** 218 (1984).
6. Murrell, L. L., and Yates, D. J. C., *in* "Proceedings, 7th International Congress on Catalysis" (T. Seiyama and K. Tanabe, Eds.), Part B, p. 1470. Elsevier, Amsterdam, 1981.
7. Baliková, M., and Beránek, L., *Collect. Czech. Chem. Commun.* **40,** 3108 (1975).
8. Yuen, S., Chen, Y., Kubsh, J. E., Dumesic, J. A., Topsøe, N., and Topsøe, H., *J. Phys. Chem.* **86,** 3022 (1982).
9. Hobson, M. C., Jr., and Gager, H. M., *J. Colloid Interface Sci.* **34,** 357 (1970).
10. Blomquist, J., Csillag, S., Moberg, L. C., Larsson, R., and Rebenstorf, B., *Acta. Chem. Scand. Ser. A* **33,** 515 (1979).
11. Arnold, D., and Hartmut, H., *Wiss. Z.-Friedrich-Schiller-Univ. Jena, Math. Naturwiss. Reihe* **25,** 843 (1976).
12. Benesi, H. A., and Winquist, B. H. C., *in* "Advances in Catalysis" (D. D. Eley, H. Pines, and P. B. Weisz, Eds.), Vol. 27, p. 98. Academic Press, New York, 1978.
13. Shen, W. M., Dumesic, J. A., and Hill, C. G., Jr., *Rev. Sci. Instrum.* **52,** 858 (1981).
14. Sørensen, K., Internal Report No. 1, Laboratory of Applied Physics II, Technical University of Denmark, Lyngby, Denmark, 1972.
15. Mørup, S., Dumesic, J. A., and Topsøe, H., *in* "Applications of Mössbauer Spectroscopy" (R. L. Cohen, Ed.), Vol. 2, p. 1. Academic Press, New York, 1980.
16. Muan, A., and Osborn, E. F., "Phase Equilibria among Oxides in Steelmaking." Addison–Wesley, Reading, Mass., 1965.
17. Topsøe, H., Dumesic, J. A., and Boudart, M., *J. Catal.* **28,** 477 (1973).
18. Pichat, P., Mathieu, M.-V., and Imelik, B., *Bull. Soc. Chim. Fr.* **8,** 2611 (1969).
19. Kline, C. H., Jr., and Turkevich, J., *J. Chem. Phys.* **12,** 300 (1944).
20. Iizuka, T., Tatsumi, H., and Tanabe, K., *Aust. J. Chem.* **35,** 919 (1982).
21. Chu, C. T-W., and Chang, C. D., *J. Phys. Chem.* **89,** 1569 (1985).
22. Garten, R. L., Gallard-Nechtschien, J., and Boudart, M., *Ind. Eng. Chem. Fundam.* **12,** 299 (1973).
23. Segawa, K-I., Chen. Y., Kubsh, J. E., Delgass, W. N., Dumesic, J. A., and Hall, W. K., *J. Catal.* **76,** 112 (1982).
24. Garten, R. L., Delgass, W. N., and Boudart, M., *J. Catal.* **18,** 90 (1970).
25. Delgass, W. N., Garten, R. L., and Boudart, M., *J. Phys. Chem.* **73,** 2970 (1969).
26. Fitch, F. R., and Rees, L. V. C., *Zeolites* **2,** 33 (1982).
27. Dickson, B. L., and Rees, L. V. C., *J. Chem. Soc. Faraday Trans. 1* **70,** 2038 (1974).
28. Pauling, L., "The Nature of the Chemical Bond," 3rd ed. Cornell Univ. Press, Ithaca, N.Y. 1960.